

Phase transition of parallelizability in assembly systems

Ikumi Kobayashi and Shin-ichi Sasa

Department of Physics, Kyoto University, Kyoto 606-8502, Japan

(Dated: April 1, 2024)

We propose a phase transition on the feasibility of efficient parallel assembly. By introducing the parallel efficiency that measures how efficiently the parallel assembly works, the parallelizable phase is defined by its positive value. The parallelizable/unparallelizable transition is then identified by the non-analytic change in the parallel efficiency from a positive value to zero. We present two analyzable models to demonstrate this phase transition in the limit of infinite system size.

Introduction.— In industry and applied science, there are often situations where a large number of parts are assembled to make a complex product. Typical examples are automotive assembly and polymer synthesis. Recently, the advancement of nanotechnology [1] has made it possible to assemble nanoscale objects into desired structures [2–5]. Furthermore, control of polymer sequences [6, 7] and assembly of colloidal particles [5, 8–12] have been vigorously studied.

We use the term parallelization to describe simultaneously assembling subunits and then combining them to complete the final product. Parallelization increases assembling efficiency. The concept of parallelization has been studied in computer science [13, 14]. Some problems can be efficiently solved by parallel computing, whereas others cannot [15]. Inspired by these studies, we explore analogous concepts in physical assembly work. Specifically, we aim to determine under what conditions efficient parallel assembly is feasible.

The feasibility of parallelization qualitatively changes the time required for assembly. When the number of parts L becomes large, the L -dependence of the number of parallel steps d required for assembly is crucial. For example, when assembling hundreds to thousands of parts, the assembly time is drastically different depending on whether $d = \mathcal{O}(\log L)$ or $d = \mathcal{O}(L^\alpha)$.

In this Letter, we propose a phase transition called *parallelizability transition*, where parallelizable/unparallelizable phases are characterized by parallel efficiency. That is, when a system parameter is continuously changed, parallel efficiency exhibits a transition from a positive value to zero in the limit of infinite system size. We demonstrate this phase transition by presenting two analyzable models. In the first model, the quenched combinability model, one-dimensional chains are assembled in the smallest number of parallel steps. In the second model, the ANP model, a final product is assembled through random bonding reactions. We introduce the parallel efficiency to measure how efficiently the parallel assembly works. Then, we exactly show that both models exhibit the parallelizability transition.

Setup of the quenched combinability model.— Let us consider the assembly work of connecting L different parts to create a single chain. An external operator

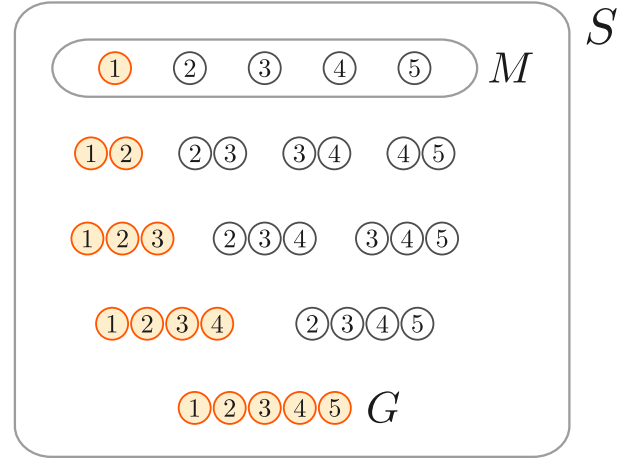


FIG. 1. All elements of S in the case $L = 5$. The final product G is placed at the bottom. The set of possible states S is the entirety of the connected subgraphs of G . The initial parts set M is shown at the top.

tries to perform the most efficient parallel assembly possible. However, the components do not always fit together. Which pairs of states can be combined is predetermined and does not change during the assembly process. The quenched combinability model idealizes such a situation.

The final product G is a one-dimensional chain [16] with L vertices. The set of possible states S is the entirety of the connected subgraphs of G . The initial parts set M is the set of states with a single vertex. The case $L = 5$ is shown in Fig. 1.

Each state $s \in S$ is either active (filled circles in Fig. 1) or inactive (open circles in Fig. 1). This active/inactive distinction represents the bonding properties of the state with other states. That is, active states can always combine with other states, while inactive-inactive pairs can combine with probability p . Initially, only the leftmost vertex of M (the vertex labeled ‘1’ in Fig. 1) is active, and the other elements of M are inactive. Then, the set of allowed bondings \hat{R} is determined probabilistically according to the following rules. For each nearest-neighbor pair of states (s_1, s_2) ($s_1, s_2 \in S$), (i) if either s_1 or s_2 is active, $(s_1, s_2) \in \hat{R}$ with probability 1 and the product is also active; (ii) if both s_1 and s_2 are inactive, $(s_1, s_2) \in \hat{R}$ with probability p and the product is also inactive. These

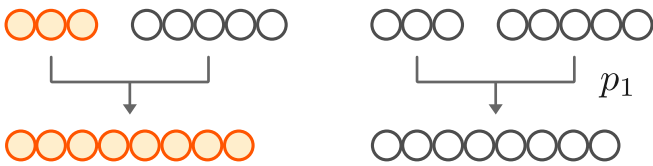


FIG. 2. Schematic of the decision procedure for the set of possible bondings \hat{R} .

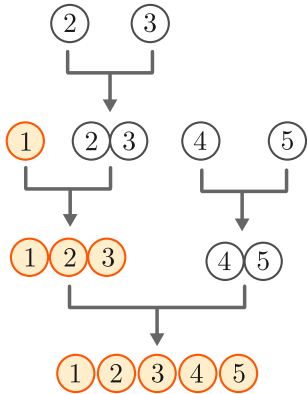


FIG. 3. One example of an assembly pathway generating an $L = 5$ chain with three parallel steps. The final product G is placed at the bottom. All the state-to-state connections in the diagram are elements of \hat{R} . The elements of M are placed at the top.

rules are illustrated in Fig. 2. This procedure determines whether the two states s_1 and s_2 can be combined.

We measure the least number of parallel steps \hat{d} required to assemble the final product G . Let us call a diagram like Fig. 3 an assembly pathway. Then, the number of parallel steps is the height of the assembly pathway. Assembly pathways must satisfy the following three conditions: (i) the final product G is placed at the bottom, (ii) all connections between states are elements of \hat{R} , and (iii) all elements of the initial parts set M are placed at the top. One example of an assembly pathway generating an $L = 5$ chain with three parallel steps is shown in Fig. 3. Among all the possible assembly pathways, we find the one with the smallest number of parallel steps and set its value to \hat{d} . The set of allowed bondings \hat{R} is probabilistically determined. Therefore, \hat{d} is also a random variable.

We introduce the parallel efficiency η to characterize the feasibility of the efficient parallel assembly. The parallel efficiency η is defined as

$$\eta := \frac{\log_2 L}{\langle \hat{d} \rangle}, \quad (1)$$

where L is the system size and $\langle \hat{d} \rangle$ is the average minimum number of parallel steps. The quantity η can be used to measure the efficiency of parallel assembly in this system because it satisfies the following two properties.

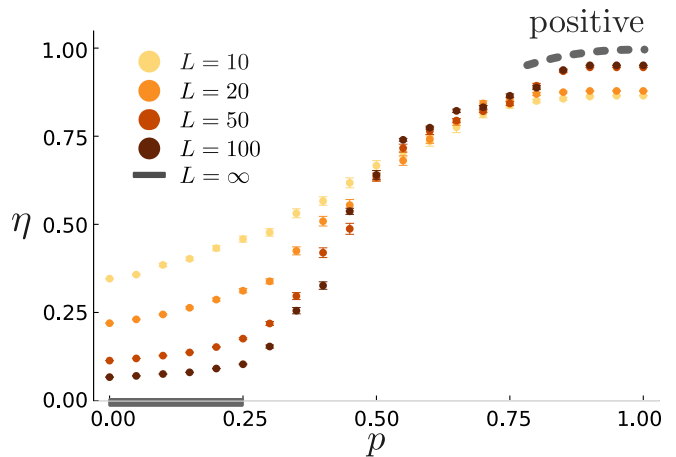


FIG. 4. Simulation results for $L = 10, 20, 50,$ and 100 in the quenched combinability model. For each p , we took 100 samples and calculated the mean and standard deviation of η . The schematic of parallel efficiency η in the limit of infinite system size is overlaid. The dashed line represents qualitative behavior. A rigorous analysis shows that the analyticity of η is broken at a point p_c satisfying $1/4 \leq p_c < 3/4$.

First, η satisfies the normalization condition $0 \leq \eta \leq 1$. Second, by checking whether $\lim_{L \rightarrow \infty} \eta$ is positive or zero, we can determine the feasibility of efficient parallel assembly in the limit of infinite system size. If the assembly process is sufficiently parallelized and $\langle \hat{d} \rangle \sim \log L$, then $\lim_{L \rightarrow \infty} \eta$ takes a positive value. In contrast, if the parallelization breaks down and $\langle \hat{d} \rangle$ grows faster than $\log L$, then $\lim_{L \rightarrow \infty} \eta$ becomes zero.

Results for the quenched combinability model.— We first display the numerical results in Fig. 4. Although the data suggest the existence of a phase transition, it is quite difficult to perform the numerical calculation for a larger system. Nevertheless, we have a rigorous proof for the existence of the phase transition [17] when L becomes infinite. We can show

$$\lim_{L \rightarrow \infty} \eta = 0 \quad (2)$$

for $0 \leq p < 1/4$, and

$$\lim_{L \rightarrow \infty} \eta \neq 0 \quad (3)$$

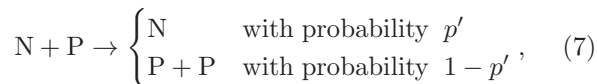
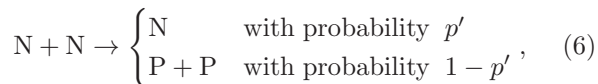
for $3/4 \leq p \leq 1$. Thus, the analyticity of η is broken at a point p_c satisfying $1/4 \leq p_c < 3/4$. This result is illustrated in Fig. 4. A rigorous proof of Eqs. (2) and (3) is given in the companion paper [17]. The breaking of the analyticity of η allows us to identify the parallelizable/unparallelizable phases without arbitrariness. In other words, the region of p satisfying $\lim_{L \rightarrow \infty} \eta \neq 0$ is identified as a parallelizable phase and the region of p satisfying $\lim_{L \rightarrow \infty} \eta = 0$ as an unparallelizable phase.

Setup of the ANP model.— Instead of optimizing the assembly pathways, we study typical pathways of

stochastic evolution of assembly in the second model. This model is interpreted as a mean-field version of the first model. To simplify the analysis, inactive states in the quenched combinability model are further classified into neutral states and passive states in the ANP model. That is, each component takes one of three states: active, neutral, or passive. In the quenched combinability model, once it is determined that two states s_1 and s_2 cannot combine, they will never combine during the assembly process. The ANP model incorporates this effect by assuming that passive states never combine with each other.

The stochastic assembly rule is as follows. Initially, there are one active and $(L - 1)$ neutral components. The assembly of the components proceeds in a repetition of the following two steps: (i) randomly pair two components as possible [18]; (ii) for each pair, perform the following bonding reaction: an active component can bond with any other component, a neutral component can bond with inactive components with probability p' , and a passive component cannot bond with passive components. If a neutral component fails to bond, the component becomes passive. We define the set of operations (i) and (ii) as a single round.

The ANP model is expressed symbolically by denoting active, neutral, and passive components as A, N, and P, respectively. Operation (ii) is then written as the following set of chemical reactions:



This procedure is illustrated in Fig. 5.

We measure the number of rounds \hat{d}' until all parts are connected. The assembly of five parts in three rounds is shown in Fig. 5. The bonding reactions occur probabilistically, and the number of rounds required to connect all the parts varies from trial to trial. Therefore, \hat{d}' is a random variable.

We introduce the parallel efficiency η' to characterize the feasibility of the efficient parallel assembly. The parallel efficiency η' is defined as

$$\eta' := \frac{\log_2 L}{\langle \hat{d}' \rangle}, \quad (9)$$

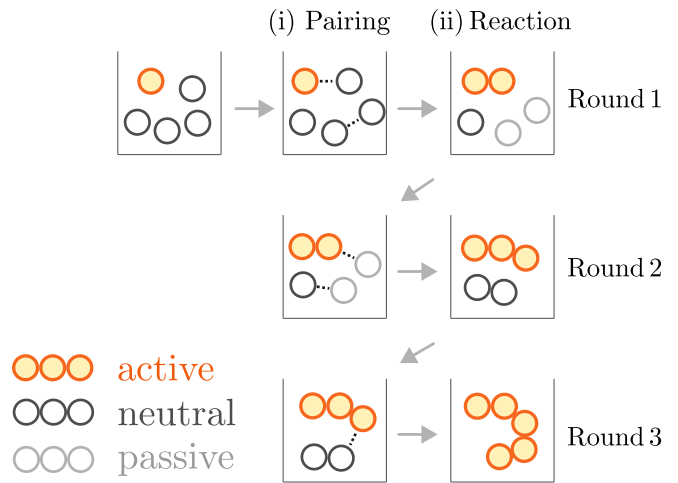


FIG. 5. Schematic of the assembly of five parts in three rounds ($L = 5, \hat{d}' = 3$). Initially, there are one active and $(L - 1)$ neutral components. A single round consists of the following two steps: (i) Randomly pair two components as possible, (ii) For each pair, perform the reactions shown in Eqs. (4)-(8). The quantity \hat{d}' is the number of rounds until there is only one component.

where L is the number of parts and $\langle \hat{d}' \rangle$ is the average number of required rounds. In a way similar to the first model, η' satisfies the following two properties. First, η' satisfies the normalization condition $0 \leq \eta' \leq 1$. Second, we can determine the feasibility of efficient parallel assembly by checking whether η' is positive or zero in the limit $L \rightarrow \infty$.

Results for the ANP model.— The simulation results are shown in Fig. 6. These graphs suggest that a discontinuous transition exists at a point p'_c . Indeed, for this model, we prove that the parallel efficiency η' has a discontinuous transition when L becomes infinite. Quantitatively, we show

$$\lim_{L \rightarrow \infty} \eta' = 0 \quad (10)$$

for $0 \leq p' < 8/9$, and

$$\lim_{L \rightarrow \infty} \eta' \neq 0 \quad (11)$$

for $8/9 < p' \leq 1$. This implies that the parallel efficiency η' is discontinuous at $p'_c = 8/9$.

The proof is the following. Let a_n , b_n , and c_n be the population of A, N, and P in the n th round, respectively. The total population of components is

$$T_n = a_n + b_n + c_n. \quad (12)$$

Because the population of A does not change through the reactions, $a_n = 1$ always holds. Assuming that L is large enough, we analyze the behavior of the expected values of b_n , c_n , and T_n ignoring terms of $\mathcal{O}(1)$. Let $\langle \hat{S}_n \rangle$ be the

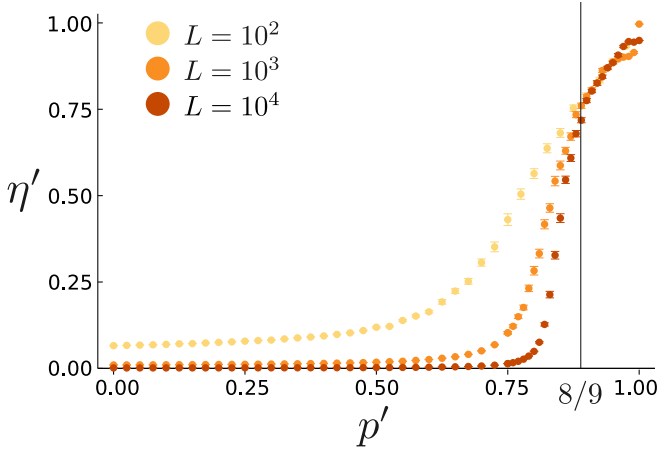


FIG. 6. Simulation results for the ANP model. For each p' , we took 100 samples and calculated the mean and standard deviation of η' . The data points approach the line $p' = 8/9$ as L increases.

expected number of P – P pairs in the n th round. We obtain

$$\langle \hat{S}_n \rangle \simeq \frac{T_n}{2} \left(\frac{c_n}{T_n} \right)^2, \quad (13)$$

where the symbol \simeq represents an approximation ignoring the terms of $\mathcal{O}(1)$ [19]. For each pair described by Eq. (6) or Eq. (7), N is generated with probability p' . Therefore, we obtain

$$\begin{aligned} b_{n+1} &= \left(\frac{T_n}{2} - \langle \hat{S}_n \rangle \right) p' \\ &\simeq \frac{T_n}{2} \left(1 - \left(\frac{c_n}{T_n} \right)^2 \right) p'. \end{aligned} \quad (14)$$

Because the number of components is halved in the reaction that produces A or N, we obtain

$$T_{n+1} = T_n - (a_{n+1} + b_{n+1}) \simeq T_n - b_{n+1}. \quad (15)$$

By setting

$$q_n := 1 - \left(\frac{c_n}{T_n} \right)^2, \quad (16)$$

we obtain

$$b_{n+1} \simeq \frac{T_n}{2} q_n p', \quad (17)$$

$$T_{n+1} \simeq \left(1 - \frac{q_n p'}{2} \right) T_n. \quad (18)$$

Substituting Eqs. (12), (17), and (18) into Eq. (16), we obtain

$$q_{n+1} \simeq \frac{q_n p' \left(1 - \frac{3}{4} q_n p' \right)}{\left(1 - \frac{1}{2} q_n p' \right)^2}. \quad (19)$$

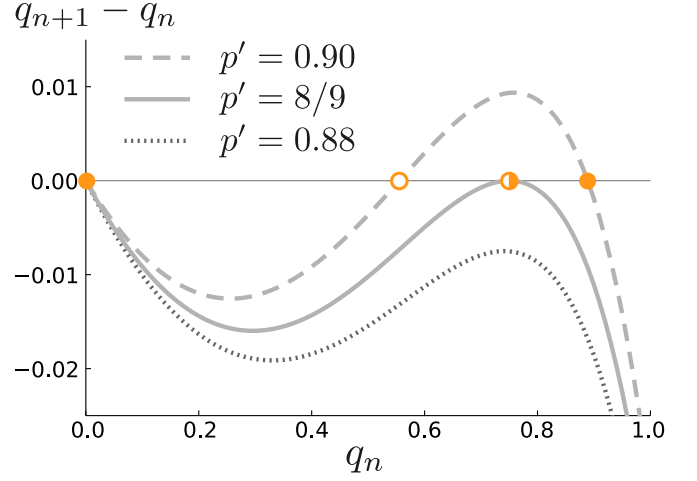


FIG. 7. Saddle node bifurcation exhibited by the discrete dynamical system of Eq. (19). When p' is less than $8/9$, only $q_n = 0$ is a stable fixed point. When p' is greater than $8/9$, a new stable fixed point and an unstable fixed point appear in $0 < q_n < 1$.

The discrete dynamical system given by Eq. (19) exhibits a saddle node bifurcation as the parameter p' changes. This bifurcation structure is shown in Fig. 7. When p' is less than $8/9$, only $q_n = 0$ is a stable fixed point. The assembly cannot be completed with $\hat{d}' = \mathcal{O}(\log L)$ because $T_{n+1}/T_n \simeq 1$. As a result, η' becomes zero in this case. In contrast, when p' is greater than $8/9$, a new stable fixed point appears in $0 < q_n < 1$. The total number of components decreases exponentially because $0 < T_{n+1}/T_n < 1$. As a result, $\hat{d}' = \mathcal{O}(\log L)$ and η' takes a positive value in this case.

Discussion.— The two models presented in this Letter characterize in-principle and realistic parallelizability, respectively. In the quenched combinability model, the pathway with the least number of parallel steps is chosen after considering all possible assembly pathways. Therefore, η characterizes whether efficient parallel assembly is feasible in principle. The equivalent situation would be bottom-up manufacturing of industrial products, where the manufacturing process is well-designed and optimized in advance. In the ANP model, L parts are randomly paired and combined, and the number of rounds until all parts are connected is measured. Therefore, η' characterizes whether efficient parallel assembly is realistically possible. The equivalent situation would be chemical synthesis, where the molecules randomly collide.

We present possible future directions. As a practical direction, this study can apply to actual industrial production processes. Parallelizable/unparallelizable transitions would emerge in connection to the success rate p of each process during the assembly of complex structures. Applying the method of this study may make it possible to calculate the threshold success rate of the elementary

process to achieve efficient parallel assembly.

As a theoretical direction, this study could lead to methods of classifying chemical reaction systems using parallel efficiency. Chemical reaction systems are classified according to the number of steady states or the number of conserved quantities [20]. Extending this study may make it possible to add another axis (parallelizable/unparallelizable) to the classification of chemical reaction systems.

The model discussed here may be realized in chemical reaction systems. In organic synthetic chemistry, chemical reactions such as living radical polymerization [21, 22] and multicomponent reactions [23, 24] are studied. Such reaction systems could correspond directly to the model analyzed in this study.

Conclusion.— In this Letter, we proposed a phase transition on the feasibility of efficient parallel assembly. We demonstrated the parallelizable/unparallelizable transition through two models. Analyzing more realistic models and generalizing the theory are future tasks.

We thank Ryohei Kakuchi, Masato Itami, Tomohiro Tanogami, and Yusuke Yanagisawa for fruitful discussions. This work was supported by KAKENHI (Grant Nos. JP19H05795, JP20K20425, and JP22H01144).

-
- [1] C. P. Poole Jr and F. J. Owens, *Introduction to nanotechnology* (John Wiley & Sons, 2003).
 - [2] K. J. Bishop, C. E. Wilmer, S. Soh, and B. A. Grzybowski, Nanoscale forces and their uses in self-assembly, small **5**, 1600 (2009).
 - [3] D. Nykypanchuk, M. M. Maye, D. Van Der Lelie, and O. Gang, DNA-guided crystallization of colloidal nanoparticles, Nature **451**, 549 (2008).
 - [4] S. Koh, Strategies for controlled placement of nanoscale building blocks, Nanoscale Res. Lett. **2**, 519 (2007).
 - [5] B. A. Grzybowski, K. Fitzner, J. Paczesny, and S. Granick, From dynamic self-assembly to networked chemical systems, Chem. Soc. Rev. **46**, 5647 (2017).
 - [6] N. Badi and J.-F. Lutz, Sequence control in polymer synthesis, Chem. Soc. Rev. **38**, 3383 (2009).

- [7] J. K. Szymanski, Y. M. Abul-Haija, and L. Cronin, Exploring strategies to bias sequence in natural and synthetic oligomers and polymers, Acc.Chem.Res. **51**, 649 (2018).
- [8] Q. Chen, S. C. Bae, and S. Granick, Directed self-assembly of a colloidal kagome lattice, Nature **469**, 381 (2011).
- [9] O. D. Velev and K. H. Bhatt, On-chip micromanipulation and assembly of colloidal particles by electric fields, Soft Matter **2**, 738 (2006).
- [10] J. J. Juárez and M. A. Bevan, Feedback controlled colloidal self-assembly, Adv. Funct. Mater. **22**, 3833 (2012).
- [11] X. Tang, B. Rupp, Y. Yang, T. D. Edwards, M. A. Grover, and M. A. Bevan, Optimal feedback controlled assembly of perfect crystals, ACS nano **10**, 6791 (2016).
- [12] F. Li, D. P. Josephson, and A. Stein, Colloidal assembly: the road from particles to colloidal molecules and crystals, Angew. Chem. Int. Ed. **50**, 360 (2011).
- [13] R. Greenlaw, H. J. Hoover, and W. L. Ruzzo, *Limits to parallel computation: P-completeness theory* (Oxford University Press on Demand).
- [14] S. Arora and B. Barak, *Computational complexity: a modern approach* (Cambridge University Press, 2009).
- [15] This is called the NC versus P problem in computational complexity theory.
- [16] In graph theory terms, G is a path graph with L vertices.
- [17] (bibliographic information of the companion regular paper), .
- [18] When the total number of components is odd, leave the extra one and do nothing until the next round.
- [19] Consider a random variable $\hat{\sigma}_i$ such that $\hat{\sigma}_i = 1$ when the i th-pair is P – P and $\hat{\sigma}_i = 0$ otherwise. Then $\langle \hat{S}_n \rangle \simeq \langle \sum_{i=1}^{T_n/2} \hat{\sigma}_i \rangle = T_n/2 \cdot \langle \hat{\sigma}_i \rangle$, and we obtain Eq. (13).
- [20] M. Feinberg, *Foundations of chemical reaction network theory* (Springer, 2019).
- [21] G. Moad, E. Rizzardo, and S. H. Thang, Toward living radical polymerization, Acc. Chem. Res. **41**, 1133 (2008).
- [22] W. A. Braunecker and K. Matyjaszewski, Controlled/living radical polymerization: Features, developments, and perspectives, Prog. Polym. Sci. **32**, 93 (2007).
- [23] R. Kakuchi, Multicomponent reactions in polymer synthesis, Angew. Chem. Int. Ed. **53**, 46 (2014).
- [24] R. Kakuchi, The dawn of polymer chemistry based on multicomponent reactions, Polym J **51**, 945 (2019).